RSC Advances

ROYAL SOCIETY OF CHEMISTRY

www.rsc.org/advances

Journal Name

RSCPublishing

ARTICLE

Sol-gel Nanocasting Synthesis of Kesterite Cu_2ZnSnS_4 Nanorods

Jing Wang, Peng Zhang*, Xuefeng Song, and Lian Gao*

Cite this: DOI: 10.1039/xoxxoooooox

Received ooth January 2012,
Accepted ooth January 2012

DOI: 10.1039/xoxxoooooox

www.rsc.org/

Nanocasting synthesis of quaternary chalcogenide Cu_2ZnSnS_4 (CZTS) nanocrystals remains a big challenge due to the difficulty in the impregnation of the quaternary precursors and the competition of the formation of binary and ternary sulfides. We herein report the first successful nanocasting synthesis of nanorods of the quaternary sulfide compound, CZTS, based on mesoporous SBA-15 template through a sol-gel process. Kesterite CZTS nanorods with a diameter of 6.8 nm and a surface area of 76.19 $m^2 g^{-1}$ are obtained. The compositions and concentrations of the quaternary precursors are investigated for the impregnation and crystallization of CZTS in the silica template.

Introduction

Cu_2ZnSnS_4 (CZTS), a natural-abundant and environment-friendly solar absorber material with high absorption coefficient, low cost, and an optimal energy band structure, has been widely researched.[1] CZTS nanocrystals with various morphologies have been synthesized via different solution-based procedures such as solvothermal[2-4] and hot injection methods[5-11]. Compared with the spherical nanoparticles, CZTS nanorods have rarely been reported using wet-chemical synthesis methods due to the relative difficulty in the control over growth direction of CZTS particles in solution. Singh *et al.*[8] reported preparation of wurtzite CZTS nanorods (11× 35 nm) by injecting 1-dodecanethiol (1-DDT) and *tert*-dodecylthiol (t-DDT) into 1-octadecene (1-ODE) solution containing metal salts and trioctylphosphine oxide (OPTO), where thiols (1-DDT and t-DDT) played a critical role in forming nanorods. After modifying the above work, wurtzite CZTS nanorods with different aspect ratios and axial composition gradients were prepared successfully.[9] Zou *et al.*[10] prepare wurtzite CZTS nanorods (diameter of 7 nm and lengths up to 30-40 nm) in either DDT or oleylamine (OLA) using dissolved elemental sulfur in octadecene (ODE-S solution) as the sulfur precursor. Relative to wurtzite structure, the kesterite CZTS is a thermodynamically stable phase. The growth of kesterite grains within a template of ordered wurtzite nanorods has been proposed to be driven by the transition from the metastable to the stable crystalline phase.[12] Single-crystalline CZTS nanorods with kesterite structure have been prepared via a solvothermal reaction at 180□ for 48 h in small scale.[4] However, the obtained CZTS crystals are composed of both nanorods (10 × 30 nm) and aggregates of small particles.

The utilization of a considerable amount of long chain organics in the hot-injection and solvothermal methods introduces organic components, *e.g.*, thiols and oleylamine, as capping ligands.[8,13] Specific treatments are often applied to remove or replace the long chain molecules with short ones for applications in solar energy conversion.[1,14] In this regard, casting methods have been applied to synthesize CZTS nanowires and nanotubes using hard templates, such as anodic aluminum oxide (AAO), to avoid the usage of capping ligands. Shi *et al.*[3] have prepared ordered single-crystalline nanowires arrays of CZTS via a solvothermal approach using AAO as a hard template, yet this reaction takes 70 hours at 230 □. Chan *et al.*[15] reported growth of CZTS nanorods using electrodeposition method in AAO template. AAO has also been applied as a template to synthesize Cu_2ZnSnS_4 nanowires and nanotubes via a modified sol-gel approach following a high-temperature sulfurization.[16] However, the as-synthesized CZTS nanostructures all possess a diameter of ~200 nm and a length of several micrometers, and the dissolution of the AAO templates in NaOH aqueous solution usually leads to corrosion of CZTS nanostructures.

The currently applied methods for preparation of CZTS nanorods either utilize high temperature wet process and long-chain organics, or use AAO template that forms kesterite nanorods with big diameters. An alternative approach with safe and simpler process for preparation of smaller and scalable kesterite CZTS nanorods is thus desired.[17] Mesoporous silica, *e.g.* SBA-15, KIT-6, have been widely applied as hard templates for preparation of a variety of nanostructured oxides, *e.g.* Fe_2O_3, $CuCrO_2$, In_2O_3.[18-20] Some binary sulfide nanocrystals, *e.g.* CdS,[21] ZnS,[22] and In_2S_3,[22] have also been reported using nanocasting methods. However, much fewer sulfide nanorods have been reported by nanocasting method relative to oxides. Cao *et al.*[21] prepared mesoporous crystalline CdS arrays by SBA-15 template using cadmium thioglycolate [$Cd_{10}S_{16}C_{32}H_{80}N_4O_{28}$] as both the Cd and S precursors. Shi *et al.*[23] fabricated highly ordered mesoporous WS_2 and MoS_2 via a high-temperature sulfurization in H_2S flow. In spite of these achievements, the synthesis of quaternary sulfides using nanocasting method has never been reported so far, to the best of our knowledge. This is mainly due to the challenge in both the uniform impregnation of the multiple precursors into the pore

channels and the difficulty in the control over nucleation and crystallization of quaternary compounds, which faces the competition of formation of binary and ternary sulfides.

Herein, we report for the first time an adjusted nanocasting method for the synthesis of kesterite CZTS nanorods with diameters smaller than 7 nm and lengths up to approximate 100 nm using mesoporous silica SBA-15 as template. This simple method avoids the usage of organic capping agents and high temperature solution. The direct annealing (320 ^{o}C) of the impregnated template in argon leads to the crystallization of the CZTS compound, which avoids the high-temperature sulfidation in toxic H_2S or S vapor. The thiourea behaves as both sulfur source and chelating agents for the uniform incorporation and crystallization of the three metal ions in the template channels.

Experimental Section

Synthesis of CZTS samples: SBA-15 was prepared according to the typical procedure as reported[24] and used as template for the nanocasting synthesis. In a typical nanocasting procedure, 0.18 g of thiourea (Tu), 0.07 g of zinc chloride ($ZnCl_2$), 0.12 g of tin (II) chloride dihydrate ($SnCl_2{\cdot}2H_2O$), and 0.13 g of copper acetate monohydrate ($Cu(Ac)_2{\cdot}H_2O$) with a precursor ratio Cu:Zn:Sn:S of 1.3:1.0:1.0:4.7 were dissolved in 5 ml methanol in sequence. The solution was then slowly added to 0.3 g SBA-15 powders with vigorous stirring for 6 h. The products were then put into a tube furnace and annealed at 320 ^{o}C for 5 h in argon flow with a heating rate of 1 ^{o}C min^{-1}. To remove the silica template, the obtained sample were treated using 10% HF solution. The precipitates were then washed with milliQ water and ethanol four times and dried at 60 ^{o}C. Black powders were finally obtained. For comparison, different samples were prepared by changing the total masses of CZTS precursor salts (0.25 g and 2.5 g) impregnated into 0.3 g SBA-15 powders via similar procedures.

Characterization of samples: The XRD patterns of the samples were identified on a X-Ray Polycrystaline Diffractometer (XRD, D8 ADVANCE, Bruker Co., LTD, Germany, Cu Kα, λ = 1.54178 Å) and the Raman spectrum was obtained on a spectrometer (Bruker Optics Senterra R200-L). Transmission electron microscopy (TEM) images of the samples were performed on JEM-2010HT analytical transmission electron microscope operated at an acceleration voltage of 200 KV. Energy-dispersive X-ray spectroscopy (EDS) of the as-obtained products were performed on INCA X-Act. The chemical binding energy of the product was measured on a Kratos AXIS Ultra DLD spectrometer. Nitrogen absorption and desorption measurements were performed on an Autosorb IQ instrument. The surface areas and pore size distributions of the samples were calculated by the Brunauer-Emmett-Teller (BET) and Barrett-Joyner-Halenda (BJH) methods, respectively. The infrared spectrum was recorded using a Fourier Transform Infrared Spectrometer (Nicolet 6700). The spectrum was collected on a potassium bromide disc in the range of 4000-400 cm^{-1}. UV-vis absorption was carried out by UV-vis spectroscopy (UV-2450). The absorbance at near IR region was collected on UV/Vis/NIR Spectrometer (Lambda 750S, Perkin Elmer, Inc., USA).

***Photoelectrochemical (PEC) measurements*:** All PEC measurements were performed using a three-electrode experimental setup (CHI660D electrochemical workstation, Chenhua, Shanghai) using a side window of a Xenon lamp (300 W, Newport 6258, USA) as a light source. A platinum wire and a saturated calomel electrode (SCE) acted as the counter and reference electrode, respectively. The Na_2SO_4 (0.2 mol L^{-1}) aqueous solution was used as electrolyte.

Results and Discussion

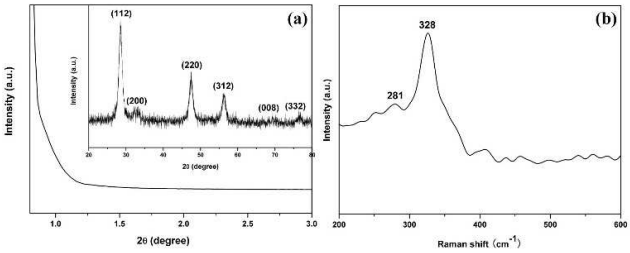

Fig. 1 (a) Small-angle XRD pattern. Inset: Wide-angle XRD pattern; (b) Raman spectrum of the prepared CZTS nanorods.

X-ray diffraction (XRD) patterns and Raman spectrum of the obtained sample, Fig. 1a and 1b, identify the production of CZTS. The diffraction peaks of wide-angle XRD pattern (inset of Fig. 1a), can be indexed to the kesterite CZTS (JCPDS, Card, no.26-0575). The broadened diffraction indicates a nanocrystalline nature of the obtained CZTS. Since the X-ray diffraction peaks are close to those of ZnS (JCPDS, Card, no.65-0309) and Cu_2SnS_3 (JCPDS, Card, no.27-0198). The information from Raman spectrum is collected to further confirm the presence of CZTS structure. The scatterings at 328 and 281 cm^{-1}, Fig. 1b, have red shifts relative to the reported bulk one, which can be attributed to the nanoscale of the CZTS particles.[25] The absence of peaks at 278 cm^{-1}, 351 cm^{-1} and 295-303 cm^{-1}, 355 cm^{-1} indicates the absence of ZnS and Cu_2SnS_3 in the sample.[26] The wide-angle XRD and Raman results confirm the main phase of CZTS for the obtained sample.

The diminish of small-angle diffraction intensity after impregnation of CZTS in the SBA-15, Fig. S1b, relative to original SBA-15 (Fig. S1a), indicates discontinuous impregnation of CZTS in channels of SBA-15. The absence of diffraction peaks in the small-angle XRD pattern of the obtained CZTS samples after removal of SBA-15, Fig. 1a, indicates the absence of ordering in the obtained sample. This is consistent with the representative TEM images of the sample in Fig. 2a and S2c. With CZTS impregnated in the channels, Fig. S2b, the ordered structure of SBA-15 template (Fig. S2a) have not been changed. After removal of silica template by HF etching, the one-dimensional feature is sustained in the CZTS products, Fig. 2b and S2c. The CZTS nanorods show a uniform diameter of ~ 6.8 nm, Fig. 2a and b, slightly smaller than the size of the template channel (9 nm). This is due to the shrinkage of the volume after formation of solid compound in the pore

channels. The length of the nanorods ranges from 20 to 100 nm. In some cases, the nanorods form continuous nanowires by attachment to each other as in Fig. 2b and S2c. The high resolution TEM (HRTEM) image of the template-free CZTS, Fig. 2c, shows clear lattice fringes with an interplanar distance of 0.31 nm, corresponding to the (112) facets. The selected area electron diffraction (SAED) pattern (inset of Fig. 2b) matches the polycrystalline structure of CZTS. The diffraction rings correspond to the (112), (220), and (312) planes, respectively. Both HRTEM and SAED indicate well crystallinity of CZTS nanorods.

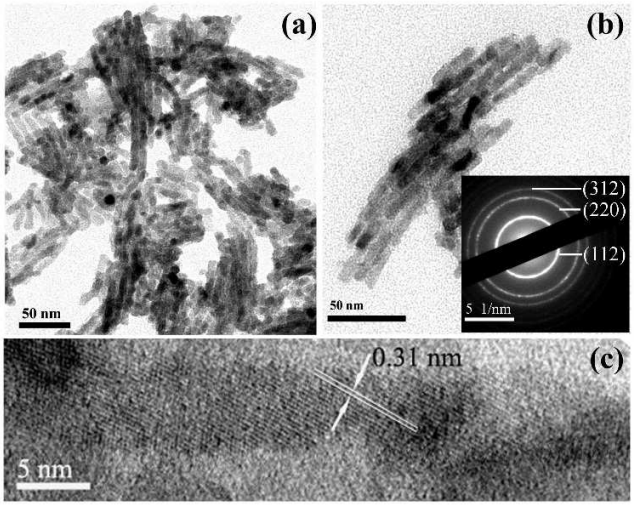

Fig. 2 (a) TEM image; (b) TEM image with higher magnification. Inset: SAED rings; (c) HRTEM image of the as synthesized CZTS nanorods.

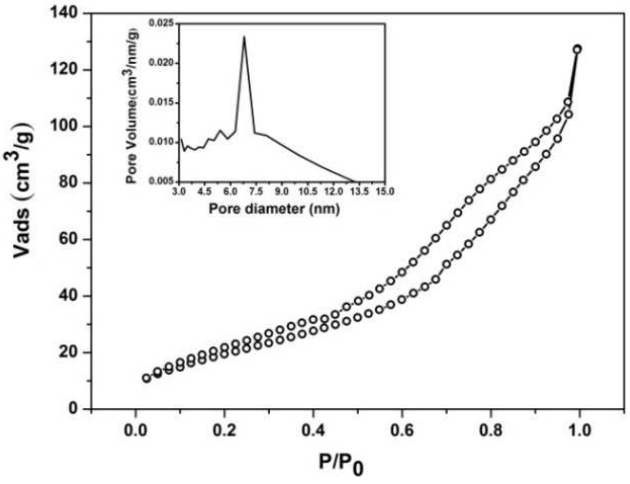

Fig. 3 N_2 adsorption-desorption isotherm of the obtained CZTS nanorods. Inset: pore size distribution calculated using Barrett-Joyner-Halenda (BJH) method.

The N_2 adsorption-desorption isotherm of the CZTS nanorods can be classified as type IV with a H_3 hysteresis loop, Fig.3. In addition, the capillary condensation range is broad with p/p_0 ranging from 0.3 to 1, which is characteristic of a high fraction of textural porosity. The pore size of ~7.0 nm agrees well with wall thickness of SBA-15. The Brunauer-Emmett-Teller (BET) surface area of the template-free CZTS is 76.19 $m^2 g^{-1}$, which is larger than the CZTS powders prepared by a modified sol-gel method (27 $m^2 g^{-1}$)[27] and surfactant-free solvothermal preparation (72 $m^2 g^{-1}$).[28]

Table 1 Five representative EDX data taken from template-free CZTS.

Element	Atomic % of 5 different locations on nanoparticles					Atomic ratio
Cu	17.02	17.47	18.26	17.17	17.53	1.25
Zn	14.28	14.95	14.05	12.10	14.73	1.00
Sn	12.99	11.83	12.70	12.61	12.74	0.90
S	62.73	62.75	62.80	65.12	65.01	4.56

The elemental stoichiometry of CZTS nanorods was measured through (EDS) analysis on five investigated spots, which shows the copper-poor and zinc-rich ratio of Cu: Zn: Sn: S = 1.25: 1.00: 0.90: 4.56, as shown in Table 1. The elemental ratio is very close to the stoichiometric ratio of the precursors (1.3: 1.0: 1.0: 4.7). This indicates well retaining and crystallization of the impregnated precursors.

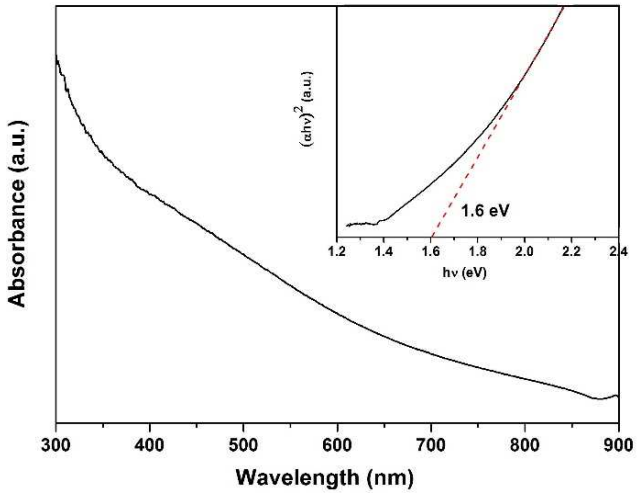

Fig. 4 UV-vis absorption spectrum of the CZTS nanorods at room temperature. Inset shows the plot of $(\alpha hv)^2$ vs. photon energy.

The UV-vis absorption spectrum of the CZTS nanorods at room temperature, Fig. 4, shows an optical band gap of 1.6 eV. The optical band gap (E_g) is estimated by plotting $(\alpha hv)^2$ as a function of the photon energy (inset of Fig. 4), where α and hv represent the absorption coefficient and the photon energy, respectively. The estimated E_g value from the intersection of the extrapolated linear portion with the x-axis (photon energy) is 1.6 eV, which is deviated from experimental results[3,29,30] but less than the theoretical value of 1.64 eV for Cu_2ZnSnS_4.[31] This can be attributed to the crystalline defects resulting from nonstoichiometric amounts of ions.[31] Besides, it verifies the absence of band gaps of ZnS (3.7 eV) and Cu_2SnS_3 (0.93 eV).[29,30]

The presence of all four constituent elements in their expected oxidation states can be confirmed by the X-ray photoelectron spectroscopy (XPS) analysis of Cu 2p, Zn 2p, Sn 3d, and S 2p core levels, Fig. 5. The peaks of Cu 2p at 930.5 and 950.4 eV, indicate Cu(I) with a peak splitting of 19.9 eV. The zinc spectrum shows two peaks locating at 1044 eV (Zn 2p1/2) and 1021 eV (Zn 2p3/2). The peak separation of 23 eV indicates the oxidation state of Zn (II). Sn (IV) is confirmed by the 8.5 eV separation of Sn 3d peaks, observed at 485.3 eV and 493.8 eV, which is close to the standard splitting of 8.4 eV. The S 2p spectrum shows two peaks at 161.5 and 162.6 eV with a separation of 1.1 eV, which is consistent with the reported sulfide phases.[5]

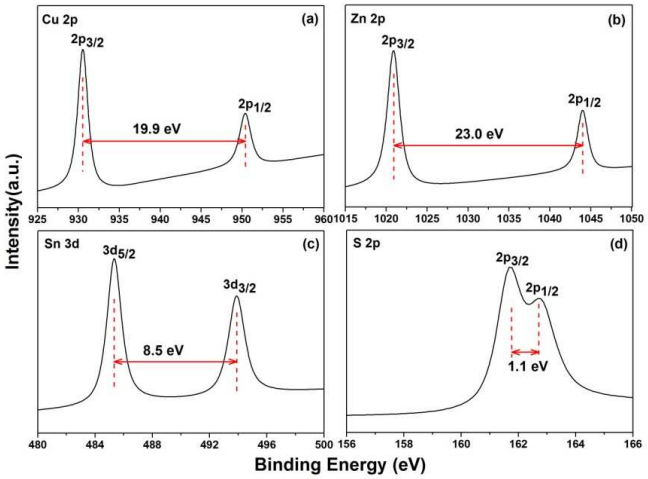

Fig. 5 XPS analysis of CZTS nanoparticles. (a) Cu 2p, (b) Zn 2p, (c) Sn 3d, (d) S 2p core levels, respectively.

FT-IR analysis on CZTS nanorods, Fig. 6, indicates the presence of surface metal-thiourea complexes. The broad band at 3442 cm^{-1} corresponds to O-H stretching vibration from the water molecule or N-H stretching vibration of thiourea. The main peaks locating at 1106, 1384, and 1631 cm^{-1} result from metal-thiourea complexes. These are consistent with the literature values with slight shift.[28] This result suggests that the thiourea has strong coordination with metal ions, considering the 320 ^{o}C annealing, HF etching, and several times washing that the obtained CZTS nanorods have undergone before FTIR measurement. In combination with the well retaining of the metal ratios in the product, the FTIR result also suggests that, in the quaternary precursor solution, the $S=C(NH_2)_2$ molecules might coordinate evenly with all three metal ions through the sulfur atoms and form $[M(Tu)_m]_n$-X_n clusters in methanol, which constitute a sol precursor solution. The M, Tu, and X here represent metal ions (Cu^{2+}, Zn^{2+}, Sn^{2+}), thiourea, and anions (CH_3COO^- or Cl^-), respectively. The tyndall effect observed in the precursor solution, Fig. S3, clearly identifies the formation of a sol. After impregnation of the sol in the template and the condensation of the sol clusters upon evaporation of solvents, the sol undergoes alcoholysis and polycondensation reactions and forms a gel in the pore channels. Subsequent annealing at 320 ^{o}C results in decomposition of the gel and crystallization of CZTS compound in the channels of the template. The strong coordination between thiourea and the metal ions in the sol clusters in the pore channels inhibits the mobility of the metal ions during crystallization and the resultant formation of binary and ternary compounds. The mobility of metal ions, *i.e.* the incompatibility of the metal ions with silica surface, is a challenging issue in nanocasting synthesis, especially for copper based compounds.[19] The presence of thiourea not only stabilizes the precursor solutions, but guaranties the crystallization of the quaternary compound in the template channels during high temperature annealing.

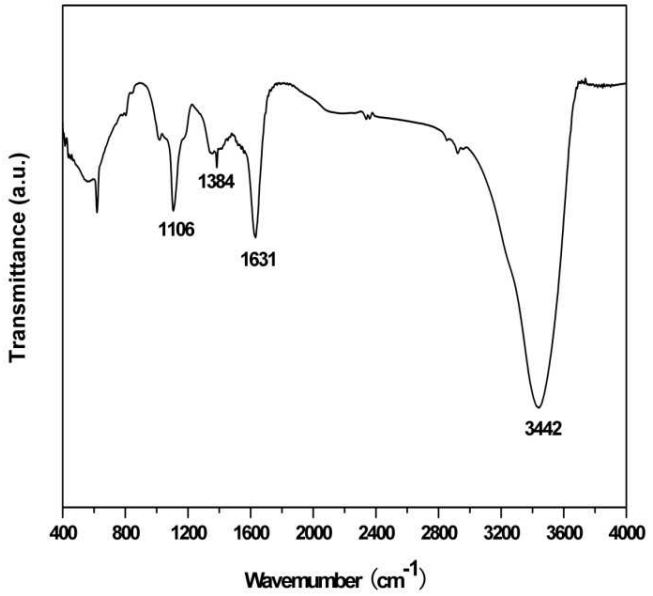

Fig. 6 Infrared spectra of CZTS nanorods in a KBr pellet. Mainly peaks at 1106, 1384, and 1631 cm^{-1} are attributed to metal-thiourea complexes. These peaks also index other vibrations accompanying with slightly shifts, for instance, ν C-S, ν C-N or NH_2 rocking vibration (1105 cm^{-1}), NH_2 rocking vibration, ν C-S stretching vibration or N-C-N stretching vibration (1415, 1401 cm^{-1}), δ N-H bending deformation (1626 cm^{-1}).

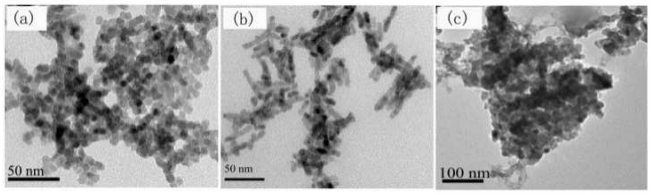

Fig. 7 TEM images of as-prepared CZTS using the same amount of SBA-15 template, which were impregnated with (a) 0.25 g, (b) a typical 0.5 g, and (c) 2.5 g of the total amounts of the precursor salts with the same molar ratios among Cu:Zn:Sn:S.

The morphologies of the as-synthesized CZTS vary with the total amounts of the precursor solution in the same amount of SBA15 template. Fig. 7a shows the TEM image of the CZTS nanocasted from 0.25 g (total mass of the four precursor salts) precursors dissolved in the same amount of solvent. Mainly nanoparticles smaller than 9 nm are observed. These nanoparticles

are loosely attached to each other forming discontinuous nanorods. This can be ascribed to the incomplete filling of the CZTS precursor in the pore channels due to the low concentration of the precursor sol. Upon calcination, the shrinkage of the solution volume in the channels makes discontinuous gels and the resultant discontinuous solid products. On the contrast, when an excess CZTS precursor, 2.5 g, is used, the over dosed sol clusters might aggregate outside the channels of template, resulting in a wide distribution of morphologies and particle sizes (Fig. 7c).

Slight adjustment on the general nanocasting procedure is necessary for the formation of CZTS nanorods. Usually, one disperses silica template powder in the precursor solution and stirs the mixture continuously into dry powers before high temperature calcination. In our experiment, we drop the precursor solution into the dry powers under constant stirring, which facilitates the capillary adsorption of the sol into the channels due to the rich availability of empty pores. The reverse process, however, will cause blocking of the pore channels due to the rich sol clusters in the solution and aggregation of sol clusters on the surface of silica particles, which leads to a wide distribution of morphologies and sizes. The resultant morphology containing template is shown in Fig. S4.

The stoichiometry of Cu_2ZnSnS_4 is tunable and deviation from the perfect elemental ratio of 2:1:1:4 has been proved to be beneficial for photoelectrochemical water splitting.[31] The stoichiometry applied in this experiment is Cu/(Zn+Sn) = 0.6, as also reported in CZTS thin films,[32,33] and located in the range of 0.4-1.0.[31] The copper poor CZTS have been more frequently reported as p-type semiconductors because Cu vacancy is the dominant acceptor defect in CZTS.[34,35] The optical absorbance in near IR region, Fig. S5, indicates the presence of rich free charge carriers as a result of the copper deficiency of CZTS nanorods, which therefore exhibit localized surface plasmon resonance (LSPR) at near IR wavelengths. [36]

Table 2 Preparation summary of CZTS methanol-based precursor solutions.

Solution	Cu precursor	Zn precursor	Sn precursor	S precursor
A	0.14 M $Cu(Ac)_2 \cdot H_2O$	0.10 M $ZnCl_2$	0.11M $SnCl_2 \cdot 2H_2O$	1.00 M thiourea
B	0.13 M $Cu(Ac)_2 \cdot H_2O$	0.10 M $ZnCl_2$	0.10 M $SnCl_2 \cdot 2H_2O$	0.47 M thiourea
C	0.23 M $CuCl_2 \cdot H_2O$	0.20 M $ZnCl_2$	0.15 M $SnCl_2 \cdot 2H_2O$	1.00 M thiourea
D	0.20 M $CuCl_2 \cdot H_2O$	0.15 M $ZnCl_2$	0.15 M $SnCl_2 \cdot 2H_2O$	0.9 M thioacetamide

During the capillary impregnation and crystallization of the quaternary compound in mesoporous template, a stable sol precursor solution is critical. Some reported precursor solutions, as have been applied in the synthesis of CZTS thin films, were also utilized for the preparation of CZTS nanorods in this study.[30,33] Besides the solution applied in this study (B in Table 2), three other types of precursor solutions (A, C, and D) were also prepared with their specific ingredients listed in Table 2. Solution A and B are both colorless and stable (for ~ 20 hours) while A is slightly turbid. Solution C is colorless and stable (for about 4 hours) when left in static state. D remains yellow and transparent for just a few minutes before precipitates appeared. Since strongly stirring results in rapid flocculation in C and D, probably due to the disturbance of the electric double layer (EDL) of colloids,[37] only solution A and B are suitable for nanocasting synthesis. When the same volume of solution A was applied as in solution B, both nanoflakes (up to 30 nm) and short nanorods (diameter of 7 nm and lengths up to 12-30 nm) were obtained (Fig. S6) and the according phases can be confirmed as CZTS (ZnS, Cu_2SnS_3) and SnS_2 by XRD (Fig. S7). The turbid nature of solution A before impregnation would be attributed to the presence of relative larger sol particles that remained outside the pores of the template and finally formed nanoflakes. The procedure in making the precursor solutions is crucial for the stability of the sol. When $ZnCl_2$, $SnCl_2 \cdot 2H_2O$, $Cu(Ac)_2 \cdot H_2O$ or $Cu(Cl)_2 \cdot 2H_2O$ are added successively to the methanol solution of thiourea or thioacetamide, rapid flocculation will not be observed. Otherwise, white precipitates will appear. This can be tentatively explained by the formation of relatively stable $[M(Tu)_m]_n$-X_n clusters or sol when the metal salts are added into thiourea solution. Further efforts need to be put in investigation of the inner mechanisms of the formation of the quaternary precursor solution, which is not the topic of this report. Anyhow, a clear and stable precursor solution is essential for the successful synthesis of CZTS nanocrystals using nanocasting method.

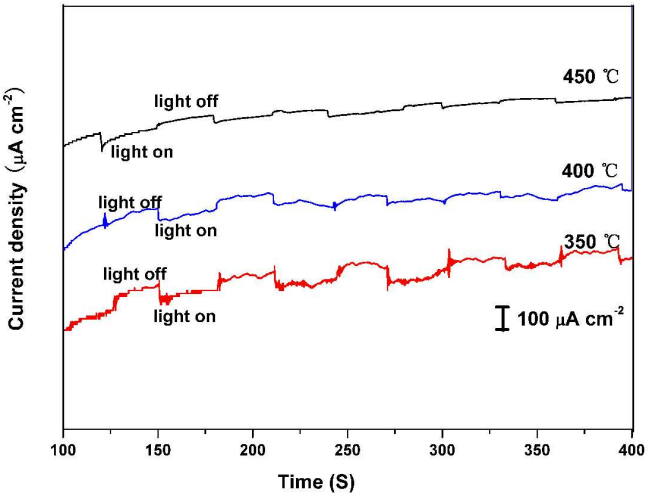

Fig. 8 Chopped I-t curves of CZTS films annealed at 350 °C, 400 °C, and 450 °C, respectively. Applied bias: -0.4 V_{RHE}; Chopped interval, 30 s; Light intensity, 10 mW cm^{-2}; Electrolyte, 0.2 mol L^{-1} Na_2SO_4 aqueous solution.

The obtained CZTS nanorods were proved to be photocatalyticly active in Na_2SO_4 solution by measurement of photocurrent density on the CZTS thin films made from nanorod powders using drop-casting method. The observed cathodic photocurrents, up to ~ 50

uA cm^{-2} under 10 mW cm^{-2} back illumination, far exceeds the ~ 3 uA cm^{-2} in Eu^{3+} solution of the CZTS thin films based on nanoparticles prepared from similar precursors.[29] Different annealing temperatures gave similar results, except that higher temperature corresponds to a lower noise level. The dark currents of the thin films are due to the high surface area of the nanorods and the poor chemical stability of the quaternary sulfides in photoelectrochemical reaction. More efforts should be put in preparation of more stable CZTS photocathode by application of surface protective layers and/or cocatalysts due to the rich pore structures of nanorods, which however is not a focus of this report. Even though the photocurrent of thin films depends strongly on preparation procedure, the much higher photoactivity of the thin films made from nanorods still indicate that nanorods are a good candidate of building blocks for solar energy conversion devices.

Conclusions

CZTS nanorods were successfully synthesized via a nanocasting method using SBA-15 template. Nanorods with diameter of 6.8 nm and lengths of approximate 20-100 nm were obtained, which corresponds to kesterite structure and a surface area of 76.19 $m^2 g^{-1}$. A sol-gel process was proposed for the crystallization of CZTS nanorods in the mesoporous template. Ingredients of precursor solution are essentially important for the successful synthesis of CZTS nanorods using nanocasting method. This method also opens a window to the preparation of polynary sulfide compounds. As-synthesized CZTS nanoparticles show higher photocatalytic activity for hydrogen production than nanoparticles prepared from similar precursors.

Acknowledgements

The authors greatly acknowledge the financial support by the National Natural Science Foundation of China (No.51172142), Opening project of State Key Laboratory of High Performance Ceramcis and Supefine Microstructure, Shanghai Municipal Natural Science Foundation (No.12ZR1414300), and the Third Phase of 211 Project for Advanced Materials Science (No. WS3116205006 and WS3116205007).

Notes and references

State Key Lab of Metal Matrix Composites
School of Materials Science and Engineering
Shanghai Jiao Tong University
800 Dongchuan Rd.
Shanghai, P. R. China 200240
E-mail: liangao@mail.sic.ac.cn, pengzhang2010@sjtu.edu.cn

Electronic Supplementary Information (ESI) available: [details of any supplementary information available should be included here]. See DOI: 10.1039/b000000x/

1 J. van Embden, A. S. R. Chesman, E. Della Gaspera, N. W. Duffy, S. E. Watkins and J. J. Jasieniak, *J. Am. Chem. Soc.,* 2014, **136**, 5237.
2 Y. L. Zhou, W. H. Zhou, M. Li, Y. F. Du and S. X. Wu, *J. Phys. Chem C,* 2011, **115**, 19632.
3 L. Shi, C. Pei, Y. Xu and Q. Li, *J. Am. Chem. Soc.,* 2011, **133**, 10328.
4 Q. Tian, X. Xu, L. Han, M. Tang, R. Zou, Z. Chen, M. Yu, J. Yang, and J. Hu, *CrystEngComm,* 2012, **14**, 3847.
5 S. C. Riha, B. A. Parkinson and A. L. Prieto, *J. Am. Chem. Soc.,* 2009, **131**, 12054.
6 Q. Guo, H. W. Hillhouse and R. Agrawal, *J. Am. Chem. Soc.,* 2009, **131**, 11672.
7 C. Steinhagen, M. G. Panthani, V. Akhavan, B. Goodfellow, B. Koo and B. A. Korgel, *J. Am. Chem. Soc.* 2009, **131**, 12554.
8 A. Singh, H. Geaney, F. Laffir and K. M. Ryan, *J. Am. Chem. Soc.* 2012, **134**, 2910.
9 M. J. Thompson, T. P. A. Ruberu, K. J. Blakeney, K. V. Torres, P. S. Dilsaver and J. Vela, *Phys. Chem. Lett.,* 2013, **4**, 3918.
10 Y. Zou, X. Su and J. Jiang, *J. Am. Chem. Soc.,* 2013, **135**, 18377.
11 W.C. Yang, C. K. Miskin, C. J. Hages, E. C. Hanley, C. Handwerker, E. A. Stach and R. Agrawal, *Chem. Mater.,* 2014, **26**, 3530.
12 R. Mainz, A. Singh, S. Levcenko, M. Klaus, C. Genzel, ; K. M. Ryan and T. Unold, *Nat Commun,* 2014, **5**, DOI:10.1038/ncomms4133.
13 A. Khare, A. W. Wills, L. M. Ammerman, D. J. Norris and E. S.Aydil, *Chem. Commun.,* 2011, **47**, 11721.
14 B. S. Tosun, B. D. Chernomordik, A. A. Gunawan, B. Williams, K. A. Mkhoyan, L. F. Francis and E. S. Aydil, *Chem. Commun.,* 2013, **49**, 3549.
15 C. P. Chan, H. Lam, K. K. Leung and C. Surya, *J. Nonlinear Opt. Phys.* 2009, **18**, 599.
16 Z. Su, C. Yan, D. Tang, K. Sun, Z. Han, F. Liu, Y. Lai, J. Li and Y. Liu, *CrystEngComm,* 2012, **14**, 782.
17 U. Ghorpade, M. Suryawanshi, S. W. Shin, K. Gurav, P. Patil, S. Pawar, C. W. Hong, J. H. Kim and S. Kolekar, *Chem. Commun.,* 2014, DOI: 10.1039/C4CC03176H.
18 X. Sun, Y. Shi, P. Zhang, C. Zheng, X. Zheng, F. Zhang, Y. Zhang, N. Guan, D. Zhao and G. D. Stucky, *J. Am. Chem. Soc.,* 2011, **133**, 14542.
19 P. Zhang, Y. Shi, M. Chi, J. N. Park, G. D. Stucky, E. W. McFarland and L. Gao, *Nanotechnology,* 2013, **24**, 345704.
20 C. Y. Ma, Z. Mu, J. J. Li, Y. G. Jin, J. Cheng, G. Q. Lu, Z. P. Hao and S. Z. Qiao, *J. Am. Chem. Soc.,* 2010, **132**, 2608.
21 F. Gao, Q. Lu and D. Zhao, *Adv. Mater.,* 2003, **15**, 739.
22 X. Liu, B. Tian, C. Yu, B. Tu, Z. Liu, O. Terasaki and D. Zhao, *Chem. Lett.,* 2003, **32**, 824.
23 Y. Shi, Y. Wan, R. Liu, B. Tu and D. Zhao, *J. Am. Chem. Soc.,* 2007, **129**, 9522.
24 D. Zhao, J. Sun, Q. Li and G. D. Stucky, *Chem. Mater.,* 2000, **12**, 275.
25 A. J. Cheng, M. Manno, A. Khare, C. Leighton, S. A. Campbell and E. S. Aydil, *J. Vac. Sci. Technol. A,* 2011, **29**, 051203.
26 L. Sun, J. He, H. Kong, F. Yue, P. Yang and *J.* Chu, *Sol. Energy Mater. Sol. Cells,* 2011, **95**, 2907.
27 L. Wang, W. Wang and S. Sun, *J. Mater. Chem.,* 2012, **22**, 6553.
28 O. Zaberca, F. Oftinger, J. Y. Chane-Ching, L. Datas, A. Lafond, P. Puech, A. Balocchi, D. Lagarde and X. Marie, *Nanotechnology,* 2012, **23**, 185402.
29 J. Wang, P. Zhang, X. Song and L. Gao, *RSC Adv.,* 2014, **4**, 27805.
30 J. Wang, P. Zhang, X. Song and L. Gao, *RSC Adv.,* 2014, **4**, 21318.

31 Y. Chen, C. H. Chuang, K. C. Lin, S. Shen, C. McCleese, L. Guo and C. Burda, *J. Phys. Chem. C,* 2014, **118**, 11954.
32 Z. Su, Ph.D. Fabrication of Cu_2ZnSnS_4 thin film solar cells via sol-gel route, *Central South University,* 2013.
33 X. Wen, W. Luo and Z. Zou, *J. Mater. Chem. A,* 2013, **1**, 15479.
34 J. M. Raulot, C. Domain and J. F. Guillemoles, *J. Phys. Chem. Solids,* 2005, **66**, 2019.
35 S. Chen, J. H. Yang, X. G. Gong, A. Walsh and S. H. Wei, *Phys. Rev. B,* 2010, **81**, 245204.
36 X. Liu and M. T. Swihart, *Chem. Soc. Rev.,* 2014, **43**, 3908.
37. Y. Zhang and T. Lv, Colloid and interface chemistry, *Chinese Textile Press, Beijing,* 2008, **11**, 214.

Keywords

Cu_2ZnSnS_4 nanocrystals, nanocasting, sol-gel, photoelectrochemistry

Jing Wang, Peng Zhang*, Xuefeng Song, and Lian Gao*

Title

Sol-gel Nanocasting Synthesis of Kesterite Cu_2ZnSnS_4 Nanorods

ToC figure

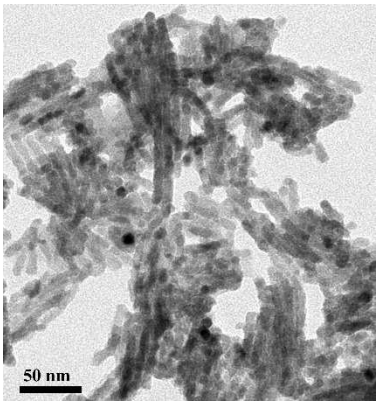

CZTS nanorods with a kesterite structure and a diameter of 6.8 nm were successfully synthesized using a nanocasting route. A sol-gel process is proposed for the impregnation and crystallization of the quaternary compound during nanocasting synthesis.